Neutron irradiation effects on the mechanical properties of powder metallurgical processed tungsten alloys

doi: 10.1016/j.jnucmat.2019.151910

Neutron irradiation effects on the mechanical properties of powder metallurgical processed tungsten alloys

Takeshi Miyazawa[1]*, Lauren M. Garrison[2], Josina W. Geringer[2], Makoto Fukuda[1,3], Yutai Katoh[2], Tatsuya Hinoki[4] and Akira Hasegawa[1]

[1]Tohoku University, Sendai, 980-8579 Japan

[2]Oak Ridge National Laboratory, Oak Ridge, TN 37831, USA

[3]Current Affiliation: National Institutes for Quantum and Radiological Science and Technology, Naka, 311-0193 Japan

[4]Kyoto University, Uji, 611-0011 Japan

Abstract

Neutron irradiation effects on the tensile properties of Pure W, K-doped W, W-3%Re, and K-doped W-3%Re were examined under the US-Japan collaboration project PHENIX. The fission neutron irradiation experiments were carried out up to 0.74 dpa at 600 °C and 800 °C. Pure W (SR) showed irradiation hardening and loss of ductility after irradiation at 600 °C and 800 °C. K-doped W-3%Re (SR) also exhibited irradiation hardening but was ductile after irradiation. Characteristic points of the K-doped W-3%Re (SR) are small grain size and layered structure. The stress-relief treatment and the layered structure may improve the ductility of powder-metallurgy W alloys after neutron irradiation, so a combination of K-doping and Re addition would be beneficial to improve irradiation resistance.

Keywords

tungsten, polycrystalline, tensile properties, neutron irradiation, thermal neutron shield

1. Introduction

Tungsten (W) is the most promising material for use as a part of plasma-facing components (PFCs) for fusion reactors (for example ITER and DEMO) because of its high melting temperature, high thermal conductivity, high resistance for sputtering, and low tritium inventory [1]. The divertor will be subjected to neutron irradiation of 14 MeV and heat flux as high as 10–20 MW/m^2 during the operation of the fusion reactor [2, 3]. The irradiation of neutrons to W causes degradation of mechanical and thermal properties, which is due to the formation of irradiation-induced defect clusters (for example, voids and dislocation loops) and irradiation-induced precipitates from displacement damage and transmutation elements [4]. Degradation of the mechanical and thermal properties may cause cracking and melting of W under unsteady operation and serious damage to the PFCs. To maintain structural soundness of divertor components, the effects of neutron irradiation on the required properties of W, including mechanical properties, must be investigated.

In order to investigate the effect of neutron irradiation on materials in fusion reactors, neutron irradiation experiments have been performed in nuclear fission reactors as there is no fusion neutron source with sufficient neutron flux. The effect of neutron irradiation interaction between solid transmutation and displacement damage needs to be clarified. The interaction between lattice atoms and neutrons depends on neutron energy. The main characteristics of the nuclear reaction between W and fission neutrons are that the neutron capture reactions are likely to occur in the thermal neutron region (E_n < 0.1 eV), and (n, p) and (n, α) reactions, on the high energy side, are less likely to occur until the energy of neutrons exceeds several MeV. Rhenium (Re) and Osmium (Os) are the main products of the transmutation process of W by the neutron capture reactions. Therefore, in water-cooled material testing fission reactors with high thermal neutron flux, the transmutation production rate of Re and Os in W is ten, to several tens of times higher than that in fusion reactors. Fission neutrons induce almost no generation

of Helium (He). Greenwood et al. [5] calculated the irradiation damage and the amount of transmutation Re and Os produced in fusion reactors, mixed spectrum reactors, and fast neutron reactors. The numerical results indicated the amount of solid transmutation elements in W differed by one to two orders of magnitude, even when irradiation damage by fast neutrons with energies of 0.1 MeV or more was the same. Therefore, this point needs to be considered when investigating the neutron irradiation effect on W, for nuclear fusion reactors, by using fission reactors. Previous studies concerning neutron irradiation effects using fission reactors reported that the amount of irradiation hardening, and the microstructure of W, differs depending on the energy spectrum of neutrons in the irradiation reactors. In our recent studies [6-9], in mixed spectrum reactors such as the High Flux Isotope reactor (HFIR) with high flux of thermal neutrons, the irradiation hardening became significantly larger when the fast neutron flux exceeded 1×10^{26} n/m^2, while in fast neutron reactors (JOYO) with low flux of thermal neutrons, irradiation hardening did not increase as much, even with the same amount of fast neutron irradiation. The main reasons are thought to be precipitation, such as σ phase (WRe) or χ phase (WRe_3) with transmuted Re, and the formation of defect aggregates such as voids or dislocation loops. Irradiation-induced segregation or precipitation also occurs under neutron irradiation, even if the amount of transmuted Re and Os is in a solid solution state in a non-irradiation environment. Therefore, these results support an irradiation study of W for fusion reactors in material testing reactors with a large number of thermal neutrons to achieve an irradiation environment with few thermal neutrons and a huge temperature range (temperatures reaching the recrystallization temperature). It was a challenge to evaluate the irradiation characteristics required for fusion reactor materials, such as tensile and impact properties, thermal properties, microstructure development, and hydrogen retention, using the same W materials.

In the US-Japan collaboration project PHENIX (PFC evaluation by tritium Plasma, HEat and Neutron Irradiation eXperiments), HFIR was used to investigate the irradiation effect on mechanical properties, thermal properties, and microstructure development due to fast neutrons between 0.4–0.7 dpa level. In order to clarify the displacement damage effect under lower transmutation conditions, a thermal neutron shield made of Gadolinium (Gd) was used inside an RB-19J capsule surrounding the specimen regions. It is reported that the Gd layer with a thickness of 1.5 mm reduced the estimated thermal neutrons flux by 1.5 to 2 orders of magnitude as compared with an unshielded capsule [10]. The RB-19J capsule of PHENIX has three subcapsules with design target temperatures of 500 °C, 800 °C and 1100 °C that were instrumentally controlled. In order to clarify the neutron irradiation effects on W, W single crystals and various types of polycrystalline W materials were examined. The results of single crystal W will be reported in a separate study by Garrison et al [11]. In this work, we will discuss a powder-metallurgical-process-sintered W polycrystalline material developed and produced from the same raw materials and using the same fabrication process. Mechanical properties of the polycrystalline W materials after neutron irradiation will also be described.

The amount of W used in a fusion reactor requires many tons of W to act as divertor tiles, even at the ITER scale. A W material can be manufactured homogeneously and can be machined at room temperature. Thus, W materials manufactured using the powder metallurgy method adopted as a material for divertor tiles of ITER are the most economic and realistic. One feature of the W materials produced by powder metallurgy is that it is possible to control the working ratio and the grain size by alloying. In particular, a layered structure in which crystal grains are flattened is formed by rolling during manufacture and, as the elastic strain is due to rolling, it should be moderated by stress-relieved treatment where the worked dislocations are partially recovered to form a cell structure consisting of dislocations in the grain [12, 13]. These microstructure controls can be effective in suppressing the low

temperature embrittlement. W is known to become brittle behavior at low temperatures. Nogami et al. reported that a reduction in the ductile-to-brittle transition temperature (DBTT) and an increase in upper shelf energy on the impact properties of W, were achieved by grain refinement in a thick plate using powder metallurgy [14]. In addition, the potassium (K)-doping or the combination of K-doping and 3%Re addition can increase the recrystallization temperature and the high temperature strengths to 1000 °C or higher [15, 16]. Grain refinement by K-doping and 3%Re addition is expected to improve the low temperature embrittlement. The K-doped W, as mentioned above, has been confirmed as an efficient method for prolonging life, such as the non-sag W of a light bulb filament [17-20]. Re addition is known to decrease the DBTT and increase high temperature strength through solid solution strengthening and softening [21]. In the case of W thick plates assuming divertor tiles of fusion reactors, a new viewpoint different from previous studies [6-9] is offered by considering the microstructural stability for three to five years in the temperature range of 1000 °C to 1300 °C (0.35 to 0.45 T_m: T_m is melting temperature (K)), and evaluating the neutron irradiation effects of the microstructure of these W materials on microstructural stability. By clarifying the properties of W materials, whose resistance to low temperature brittleness has been improved by microstructure control before neutron irradiation in the operation temperature range of fusion reactors, the purpose of this study is to understand usable operating conditions in fusion reactors from an engineering viewpoint.

2. Experimental procedures

Examined materials included in this work were Pure W, K-doped W, W-3%Re, and K-doped W-3%Re plates. These materials (supplied by A.L.M.T. corp, Japan) were fabricated using powder metallurgy and hot rolling. The reduction ratio for the hot rolling of four plates was the same. The raw plates were stress-relieved (SR) at 900 ℃ for 1.2 ks. The impurity contents in the SR plates are listed in Table 1 [22-24]. The grain structures of the examined materials were reported in the literature [24, 25]. The average grain sizes along the rolling direction (RD) and the normal direction (ND) of Pure W, K-doped W, W-3%Re and K-doped W-3%Re were 109, 38, 52 and 39 μm, respectively. The average grain sizes along the normal direction (ND) of Pure W (SR), K-doped W, W-3%Re and K-doped W-3%Re were 20, 7, 19 and 8 μm, respectively. To clarify the SR effect, recrystallized (R) Pure W and K doped W-3%Re were also prepared from the SR W materials by annealing at 1500 °C for 3.6 ks. Small tensile specimens (SS-J2) with a thickness of 0.5 mm were cut out from the plates using electro discharge machining (EDM). The gauge section of the tensile specimens was 5 mm long and 1.2 mm wide. The tensile direction was parallel to the rolling direction of the plates. The surface was mechanically polished by emery paper with a roughness of #1500.

The RB-19J irradiation campaign was conducted using a thermal neutron shield in the removable beryllium (RB) region of the HFIR at ORNL [26, 27]. The neutron irradiation conditions are listed in Table 2. Irradiation temperatures were approximately in the 600 °C and 800 °C zone, and the mean fast neutron fluences were 2.0 and 3.8 x 10^{25} n/m^2 (E_n > 0.1 MeV), respectively. A fast neutron fluence of 1 x 10^{25} n/m^2 corresponds to ~0.2 dpa in W [28]. The irradiation temperatures were monitored by thermocouples during irradiation and finally determined by examining the silicon carbide (SiC) temperature monitors of each irradiation capsule [29]. The irradiation period was 4 HFIR cycles or 8001 MWD at a nominal power of 85 MW. An RB-19J capsule is designed such that pure He is introduced at the top of the capsule

and is directed through the specimen region of each sub-capsule until it exits at the bottom of the capsule [26].

The irradiated samples were moved from hot cells for disassembling to the Low Activation Materials Development and Analysis (LAMDA) laboratory in ORNL for tensile and microhardness measurements. Before the tensile test, Vickers microhardness (HV) measurements were performed on the tab regions of the tensile specimens at room temperature, with an indentation load of 1.96 N (200 gf), and a dwell time of 15 s. At least five indents were averaged to obtain the hardness value of each sample. Tensile tests were conducted in a vacuum below 6.0×10^{-3} Pa at 500 °C and 700 °C at an initial strain rate of 1.7×10^{-3}/s by using a test frame: MTS Insight 30 at LAMDA in ORNL. A tensile test for an unirradiated specimen of Pure W (R) was conducted in a vacuum below 3.0×10^{-3} Pa at 500 °C at an initial strain rate of 1.0×10^{-3}/s by using an electromotive testing machine: CATY-T3HSt/HV13 (Yonekura MFG Co., Ltd., Japan) in Tohoku University. The tensile tests were performed without an extensometer, so the crosshead displacement was used to calculate the strain. Without extensometers, machine compliance error is present in the elastic region of the data. However, the strain and strength values in the plastic deformation region are recorded accurately. One sample was tested for each test condition. After the tensile test, fracture surfaces of the ruptured specimens were observed using scanning electron microscopy (SEM; FEI Quanta 3D 200i).

Table 1. Chemical compositions of Pure W and W alloys used in this work [22-24]

Code	Relative density (%)	Re (mass%)	K (ppm)	Al (ppm)	Si (ppm)	C (ppm)	N (ppm)	O (ppm)
Pure W	99.0	-	< 5	< 2	< 5	10	< 10	< 10
K-doped W	99.1	-	30	15	17	10	< 10	< 10
W-3%Re	98.0	3.0	< 5	2	< 5	< 10	< 10	< 10
K-doped W-3%Re	98.4	3.0	28	19	20	10	< 10	< 10

Table 2. Irradiation conditions and summary of tensile properties of irradiated W materials.

Sample ID	Material Type	Irradiation temperature [^{o}C]	Fluence [10^{25} n/m^2 (E>0.1 MeV))]	dose [dpa]	Test temperature [^{o}C]	YS [MPa]	UTS [MPa]	UE [%]	TE [%]	RA [%]
P003	Pure W (SR)	600	2.31	0.45	300	-	450	0	0	-
P000	Pure W (SR)	600	2.35	0.46	500	-	1044	0	0	0
P008	Pure W (SR)	840	3.81	0.74	500	-	1031	0	0	-
P007	Pure W (SR)	840	3.81	0.74	700	1166	1194	2.9	3.2	0
X007	Pure W (R)	830	3.80	0.74	700	-	563	-	-	0
6000	K-doped W (SR)	570	2.03	0.40	500	1205	1212	0.1	0.4	0
6008	K-doped W (SR)	790	3.66	0.71	500	1293	1325	6.0	10.1	-
6007	K-doped W (SR)	790	3.66	0.71	700	1216	1220	4.6	9.0	18
4100	W-3%Re (SR)	590	2.14	0.42	500	1233	1233	0.3	5.3	14
4109	W-3%Re (SR)	790	3.67	0.71	500	-	929	0	0	-
4108	W-3%Re (SR)	790	3.59	0.70	700	1190	1254	6.6	6.6	0
8002	K-doped W-3%Re (SR)	600	2.22	0.43	300	1470	1490	0.1	4.9	-
8000	K-doped W-3%Re (SR)	600	2.25	0.44	500	1437	1462	0.1	4.7	33
8008	K-doped W-3%Re (SR)	790	3.69	0.72	500	1374	1423	9.1	14.6	-
8007	K-doped W-3%Re (SR)	790	3.71	0.72	700	1298	1322	7.9	12.7	24
7007	K-doped W-3%Re (R)	810	3.76	0.73	700	-	907	-	-	0

3. Results

3.1. Vickers Microhardness

Figure 1 shows the irradiation hardening (ΔHV) of Pure W and its alloys, which was obtained from the difference in Vickers hardness before and after the neutron irradiation. The amount of irradiation hardening was 140–240 HV. The trend of irradiation hardening of Pure W and its alloys showed that irradiation at 600 °C and 800 °C was at almost the same level. In order to compare the irradiation hardening with previous data [6, 7], data for recrystallized Pure W irradiated in an HFIR RB-19J capsule with a thermal neutron shield and previous data for Pure W after neutron irradiation in various type reactors (HFIR unshielded, JMTR and JOYO) have been plotted in Fig. 2. Three types of Pure W samples in the existing literature were examined [6, 7, 30-35]. One of them was single crystal W, denoted as SX. The others were a rolled sheet and an arc-melted button, referred to as HR and AC, respectively. Pure W (HR) samples were annealed at the point of recrystallization heat treatment. The irradiation hardening of Pure W (R) irradiated in an HFIR RB-19J-shielded capsule was lower than that reported in literature for irradiation in an HFIR unshielded capsule. It is reported that in such an unshielded capsule at doses of 0.09–0.44 dpa (below which the intermetallic precipitation becomes apparent), nanoscale segregation of the transmutation of Re and Os was observed [36]. It is thought that the irradiation hardening was suppressed in the RB-19J-shielded capsule because a thermal neutron shield suppresses the production of Re and Os, as well as nanoscale segregation of Re and Os.

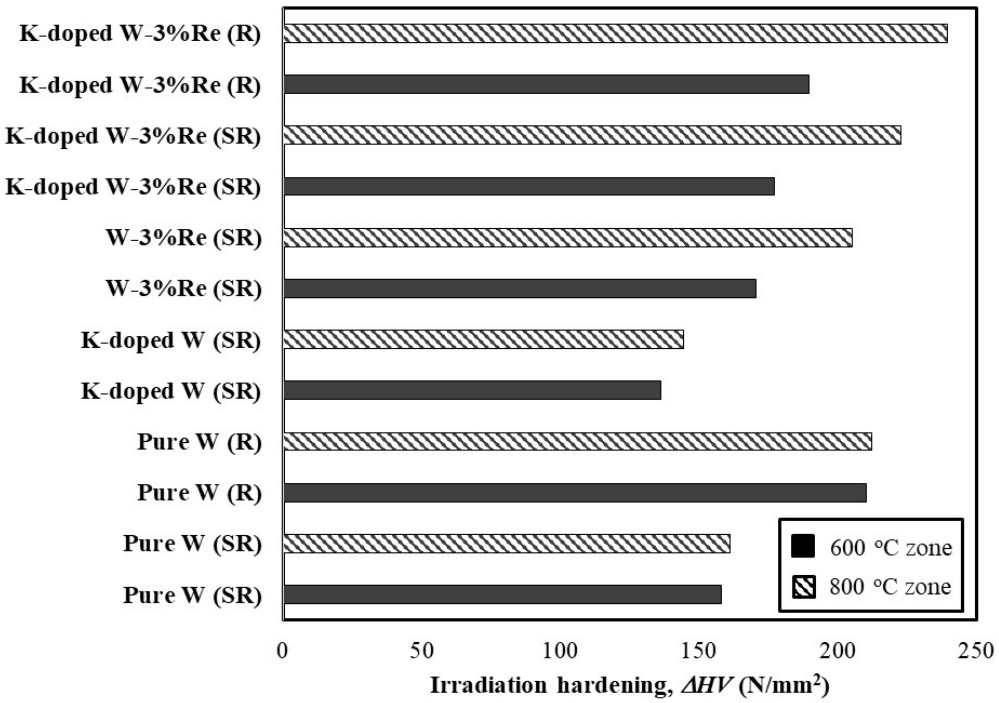

Figure 1. Irradiation hardening of Pure W and its alloys.

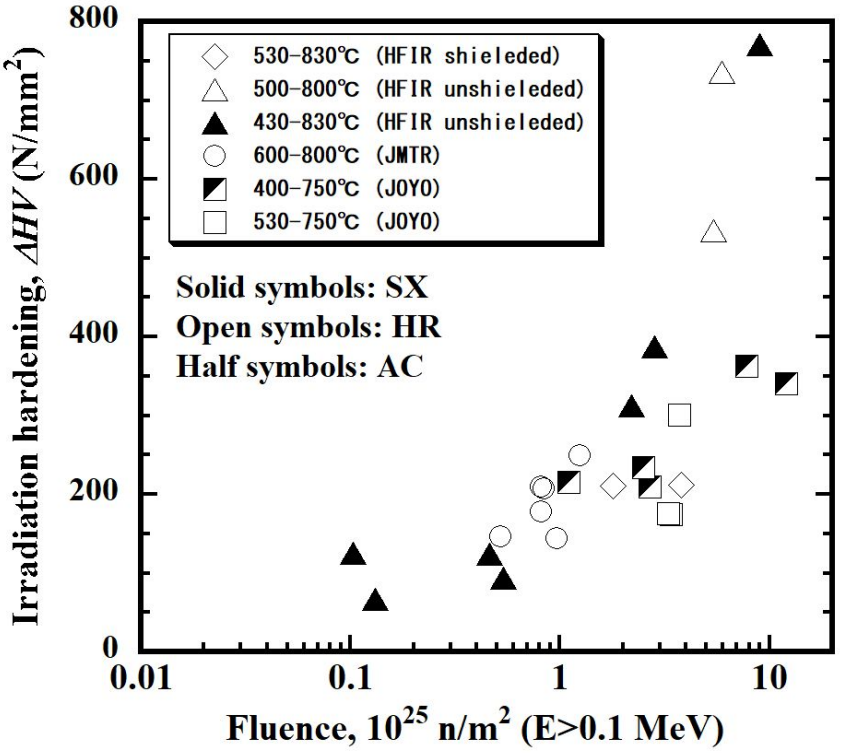

Figure 2. Dependence of irradiation hardening on fluence of Pure W [6, 7, 30-35].

3.2. Tensile Properties

Results of the tensile data for irradiated pure W and its alloys are summarized in Table 2. This includes the values of yield stress (YS), ultimate tensile strength (UTS), uniform elongation (UE), total elongation (TE), and reduction in area (RA). The RAs were estimated using fractographs of ruptured specimens.

3.2.1. Stress-Relieved W Materials

Figure 3 summarizes the engineering stress-strain curves of Pure W (SR) and its alloys (SR) before and after irradiation tested at 500 °C. Figures 4 and 5 show the ruptured surface of Pure W (SR) and its alloys (SR) tested at 500 °C. Unirradiated Pure W (SR) evidenced good elongation because the TE was 13.3%. Unirradiated Pure W (SR) had an RA of 70%, and dimples were observed on the fractographs, as shown in Fig. 5 (a), which is typical of a ductile fracture. On the other hand, the irradiated Pure W (SR) showed irradiation hardening and was ruptured in the elastic region without yielding. The ruptured surface of irradiated Pure W (SR) showed no necking, with an RA of 0%. River patterns were observed on the ruptured surface, as shown in Fig. 5 (b), which were dominated by cleavage. Irradiated Pure W (SR) showed the loss of ductility and a brittle fracture mode. K-doped W (SR) showed yielding but a small elongation, and its TE was 0.4%. However, W alloys with the addition of 3% Re (W-3%Re (SR) and K-doped W-3%Re (SR)) showed elongation. The relevant fractographs, as shown in Fig. 4 (d) and (e), show necking and dimples, evidencing a ductile fracture. Delamination of the layered structure was also observed in the ruptured surface in K-doped W-3%Re (SR). W alloys with the addition of 3% Re also showed irradiation hardening, but they exhibited ductility and plastic instability after irradiation at 600 °C.

Figures 6 and 7 show engineering stress-strain curves of pure W (SR) and K-doped W-3%Re (SR) tested at 300 °C. These curves are lower than those obtained from the materials

irradiated at 600 °C. Irradiated K-doped W-3%Re (SR) showed ductility and plastic instability at yield even at the lower temperature of 300 °C.

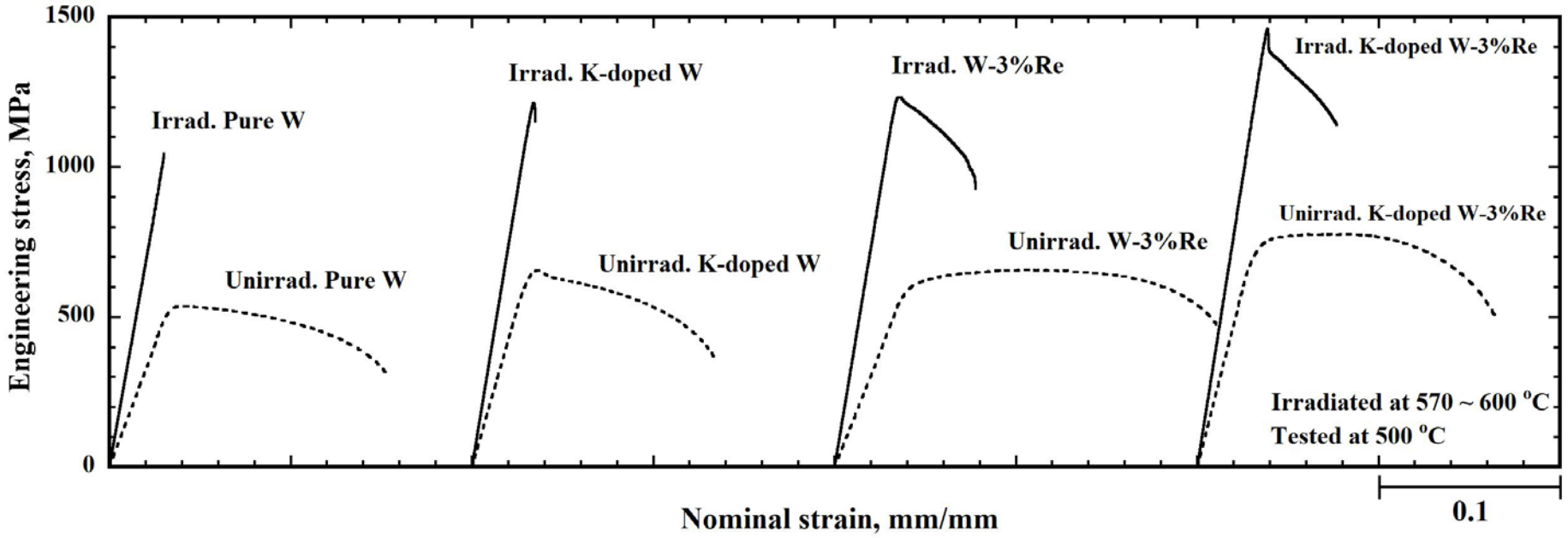

Figure 3. Stress-strain curves of Pure W (SR) and its alloys (SR) before and after irradiation tested at 500 ℃. These curves are lower than those obtained from the materials irradiated at 570-600 ºC.

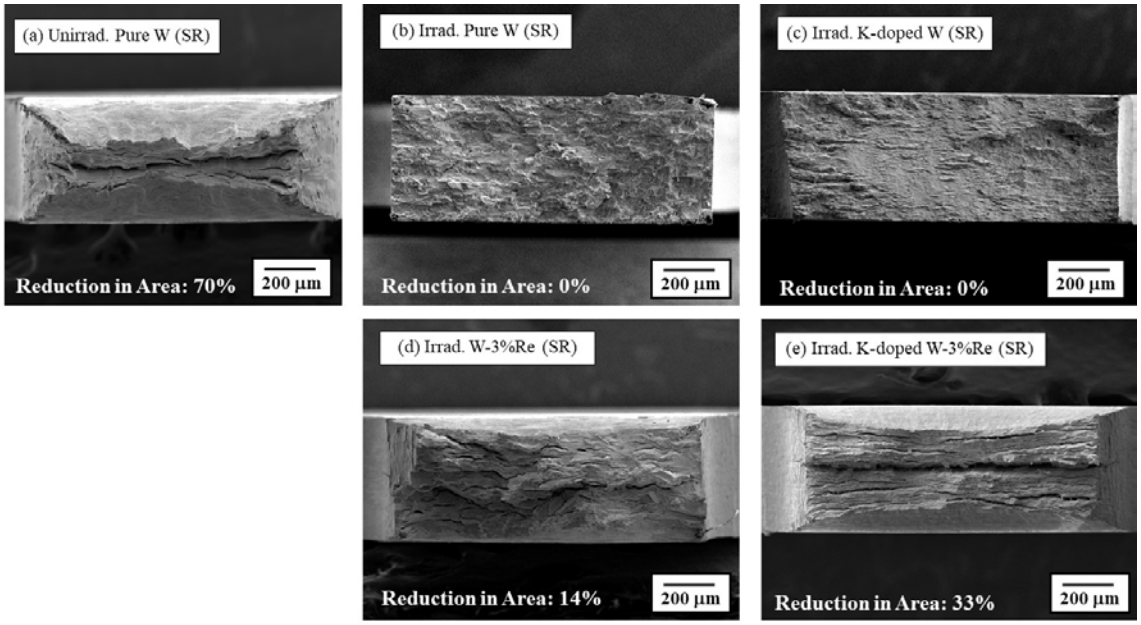

Figure 4. SEM images of the fracture surface tested at 500 °C for (a) unirradiated pure W (SR), (b) irradiated Pure W (SR), (c) irradiated K-doped W (SR), (d) irradiated W-3%Re (SR) and (e) K-doped W-3%Re (SR). Irradiation temperatures were 570–600 °C.

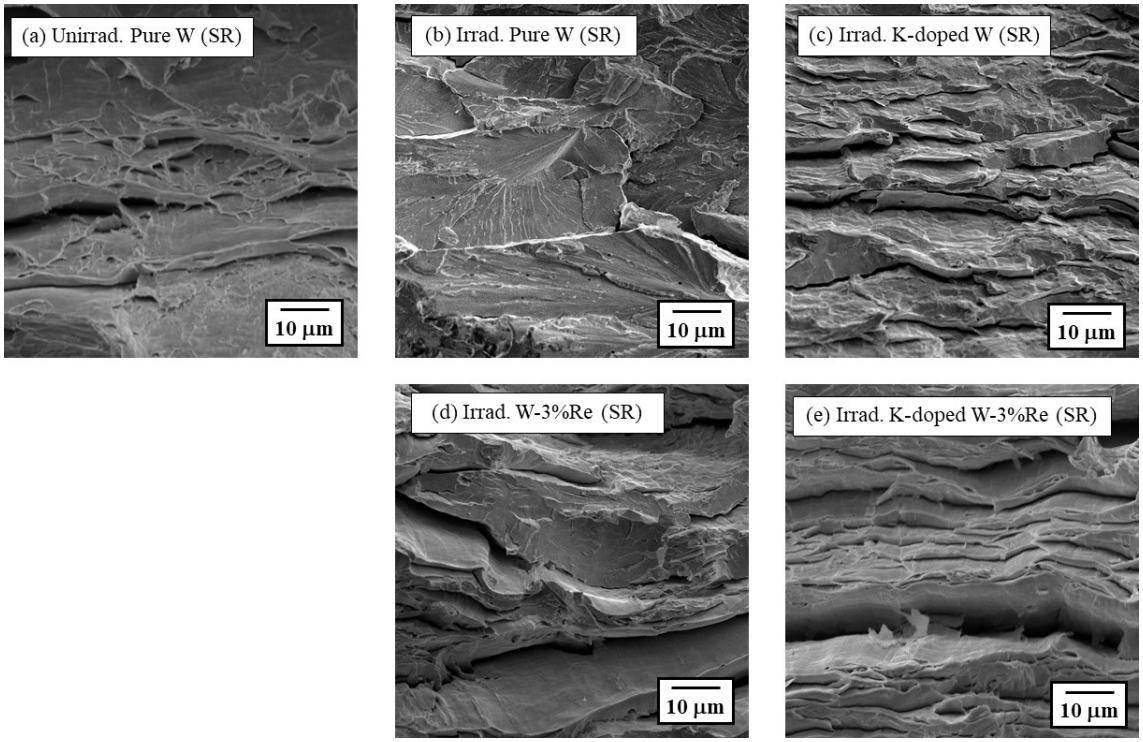

Figure 5. High magnification SEM images of the fracture surface tested at 500 °C for (a) unirradiated Pure W (SR), (b) irradiated Pure W (SR), (c) irradiated K-doped W (SR), (d) irradiated W-3%Re (SR) and (e) K-doped W-3%Re (SR). Irradiation temperatures were 570–600 °C.

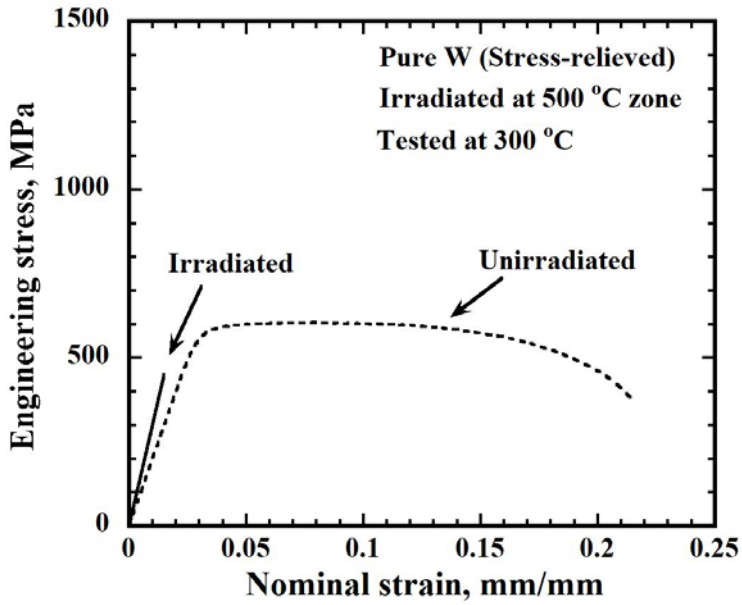

Figure 6. Stress-strain curves of Pure W (SR) tested at 300 ℃. These curves are lower than those obtained from the materials irradiated at 600 °C.

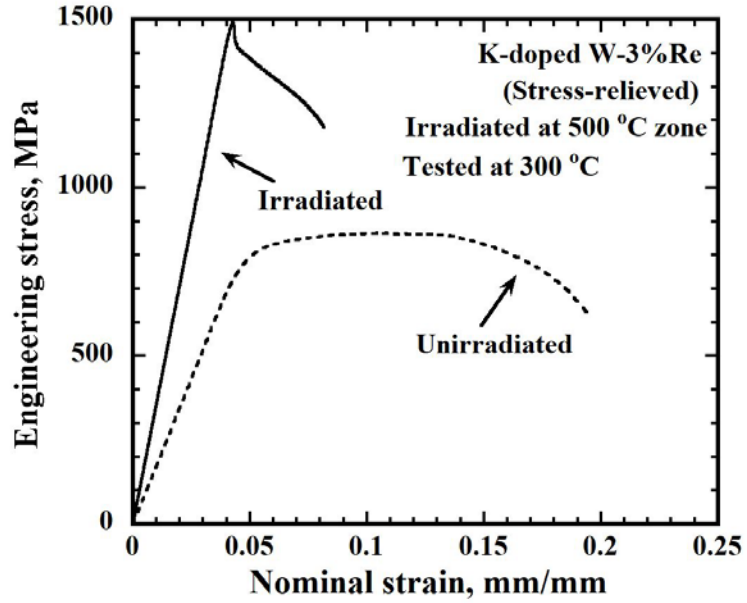

Figure 7. Stress-strain curves of K-doped W-3%Re (SR) tested at 300 °C. These curves are lower than those obtained from the materials irradiated at 600 °C.

Figure 8 summarizes the engineering stress-strain curves of Pure W (SR) and its alloys (SR) before and after irradiation tested at 700 °C. All W materials (SR) exhibited yielding but irradiated Pure W (SR) and irradiated W-3%Re (SR) fractured without necking whereas irradiated K-doped W (SR) and irradiated K-doped W-3%Re (SR) fractured due to necking. Figures 9 and 10 show the ruptured surface of Pure W (SR) and its alloys (SR). Irradiated Pure W (SR) showed yielding but the elongation was reduced after compared to before irradiation. The ruptured surface showed no necking and cleavage fracture, as shown in Figs. 9 (b) and 10 (b). Irradiated W-3%Re (SR), as shown in Figs. 8, 9 (d) and 10 (d), also showed the same tensile and fracture behavior as irradiated Pure W (SR). Irradiated Pure W (SR) and W-3%Re (SR) showed the loss of ductility and a brittle fracture mode. On the other hand, elongations of K-doped W (SR) and K-doped W-3%Re (SR) after irradiation was almost at same level to the one recorded before irradiation. The ruptured surfaces showed necking and dimples, as shown in Figs. 9 (c) (e) and 10 (c) (e). Delamination of the layered structure was also observed. The results showed that K-doped W (SR) and K-doped W-3%Re (SR) had good ductility after irradiation.

Figure 11 summarizes the engineering stress-strain curves for irradiated Pure W (SR) and its alloys (SR) when tested at 500 °C. These curves are lower than those obtained from the materials irradiated at 790–840 °C. Irradiated Pure W (SR) and W-3%Re (SR) showed typical brittle fracture behavior, while irradiated K-doped W (SR) and K-doped W-3%Re (SR) had ductility even at the lower temperature of 500 °C.

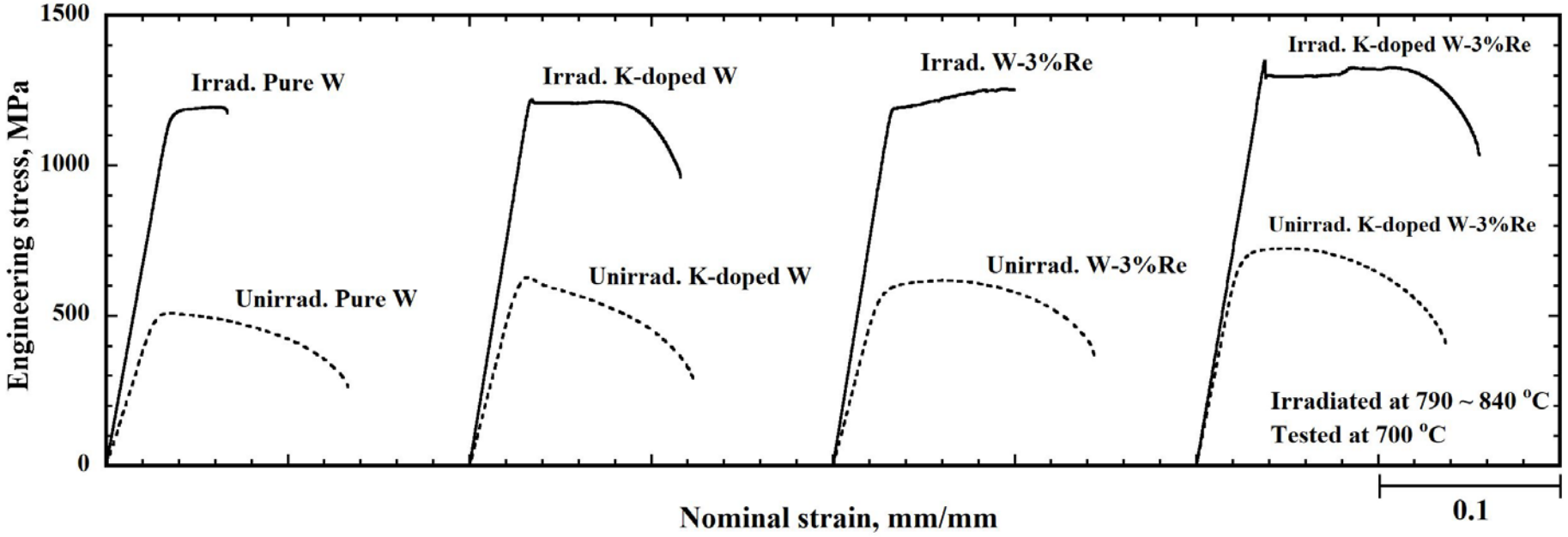

Figure 8. Stress-strain curves of Pure W (SR) and its alloys (SR) before and after irradiation tested at 700 °C. These curves are lower than those obtained from the materials irradiated at 790–840 °C.

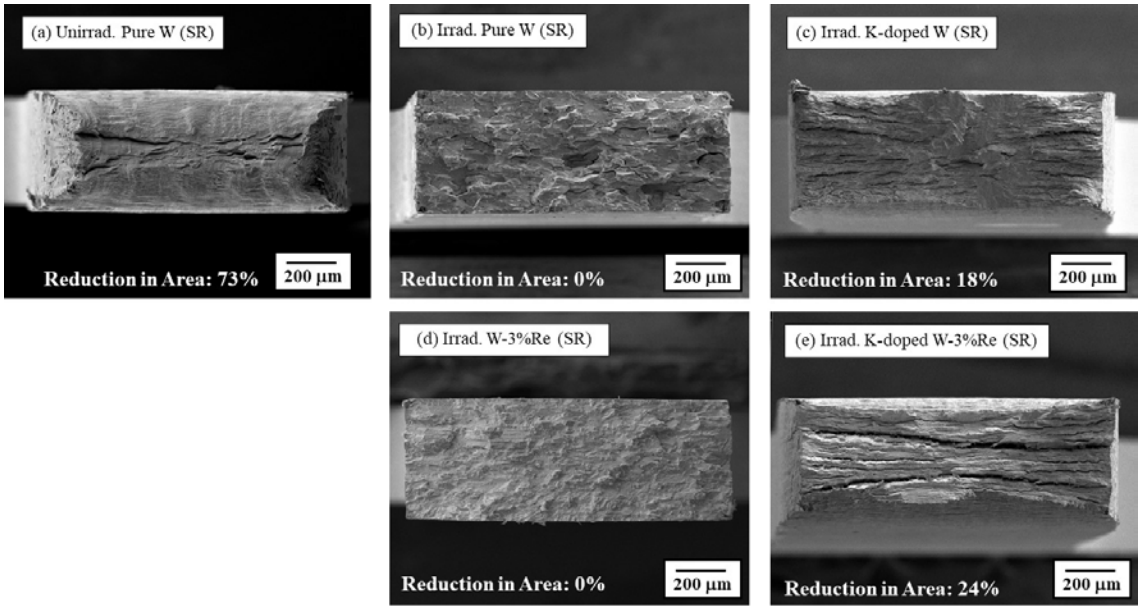

Figure 9. SEM images of the fracture surface tested at 700 °C for (a) unirradiated Pure W (SR), (b) irradiated Pure W (SR), (c) irradiated K-doped W (SR), (d) irradiated W-3%Re (SR) and (e) K-doped W-3%Re (SR). Irradiation temperatures were 790–840 °C.

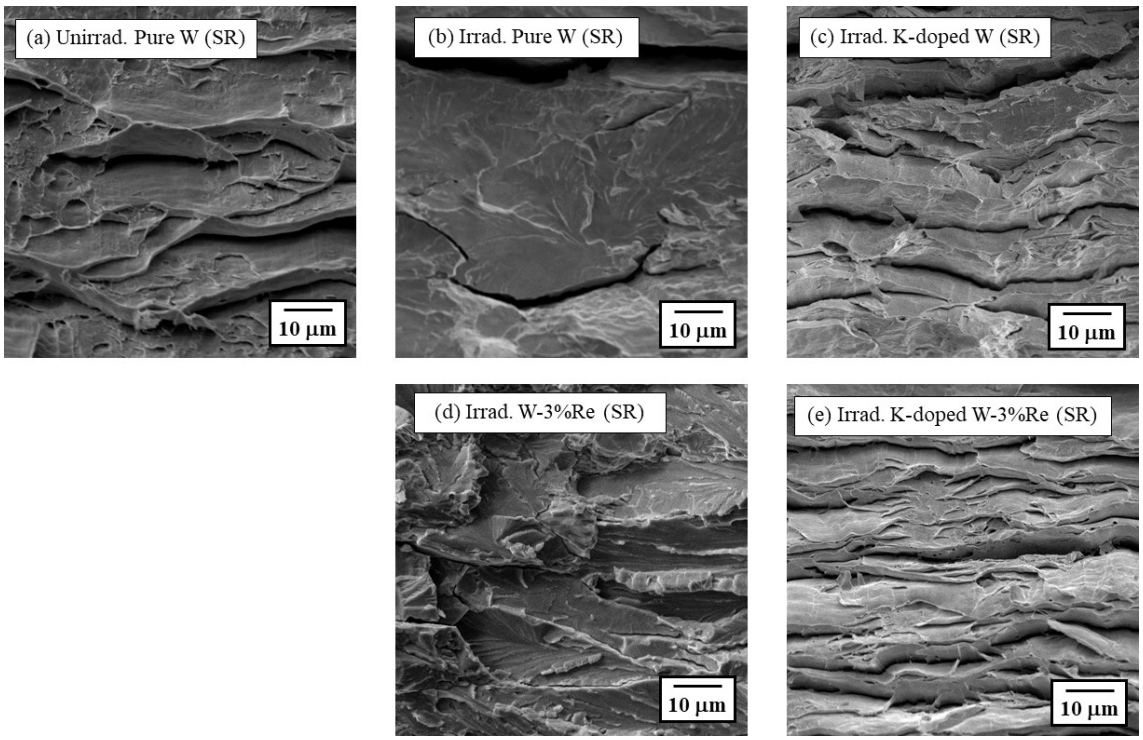

Figure 10. High magnification SEM images of the fracture surface tested at 700 °C for (a) unirradiated Pure W (SR), (b) irradiated Pure W (SR), (c) irradiated K-doped W (SR), (d) irradiated W-3%Re (SR) and (e) K-doped W-3%Re (SR). Irradiation temperatures were 790–840 °C.

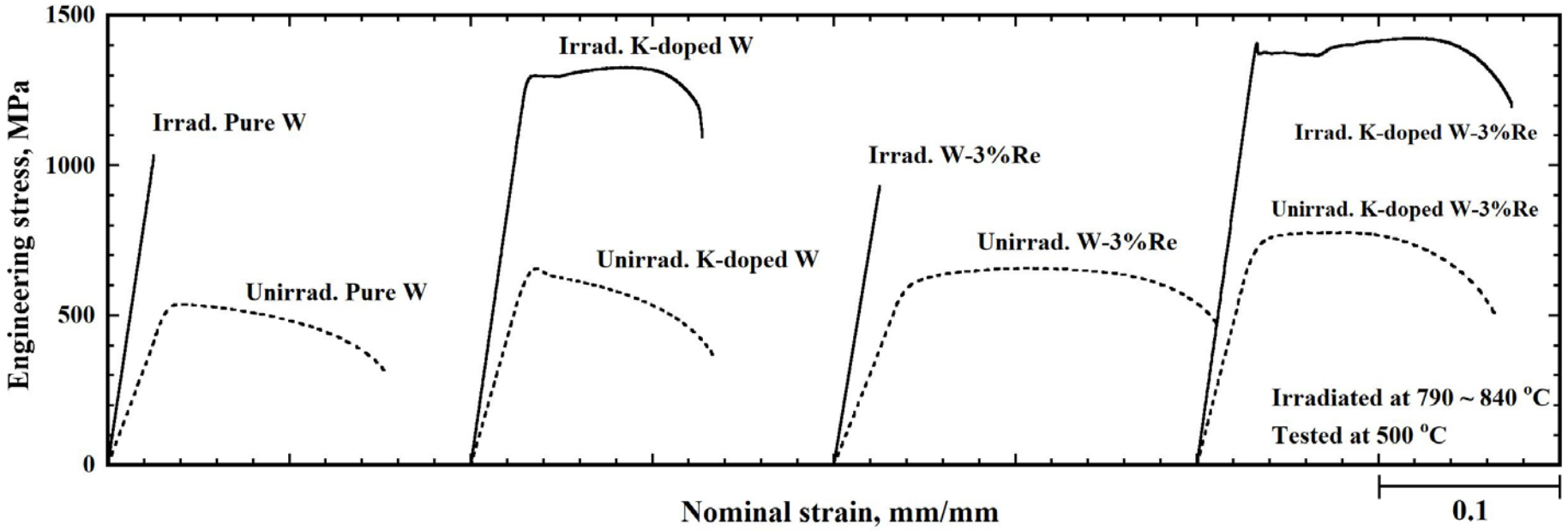

Figure 11. Stress-strain curves of Pure W and its alloys tested at 500°C. These curves are lower than those obtained from the materials irradiated at 790–840 °C.

3.2.2. Recrystallized W Materials

Figure 12 shows the engineering stress-strain curves for Pure W (R) before and after irradiation at 810–830 °C. Pure (R) before irradiation had a ductility at the test temperature of 500 °C, while irradiated Pure W (R) and irradiated K-doped W-3%Re (R) had no ductility at the test temperature of 700 °C. Both of them were fractured in the elastic region without yielding. Figure 13 shows the ruptured surface of irradiated Pure W (R) and irradiated K-doped W-3%Re (R). These ruptured surfaces showed intergranular fracture and no necking. They showed a typical brittle fracture mode. It is possible that the irradiation-induced hardening is caused by the formation of irradiation defects (voids and dislocation loops) in the matrix. As the grain interior hardens, the strength of the grain boundaries decreases and subsequently intergranular fracture occurs. Although the grain size of K-doped W-3%Re (R) was smaller than that of Pure W (R), irradiated K-doped W-3%Re (R) also showed brittle fracture behavior even when tested at high temperatures.

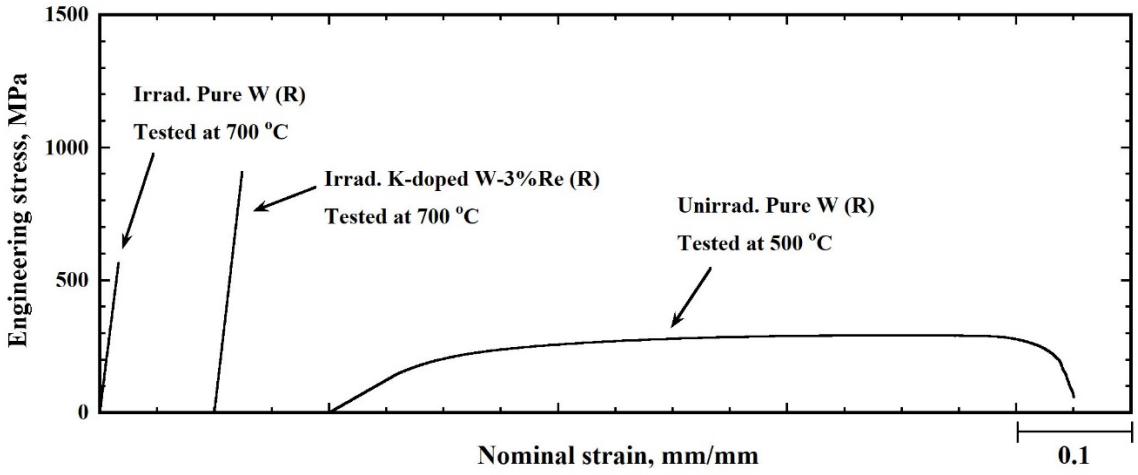

Figure 12. Stress-strain curves of unirradiated Pure W (R) tested at 500 ℃, irradiated Pure W (R) and irradiated K-doped W-3%Re (R) tested at 700 ℃, which were approximately equal to the irradiation temperature 810–830 ℃.

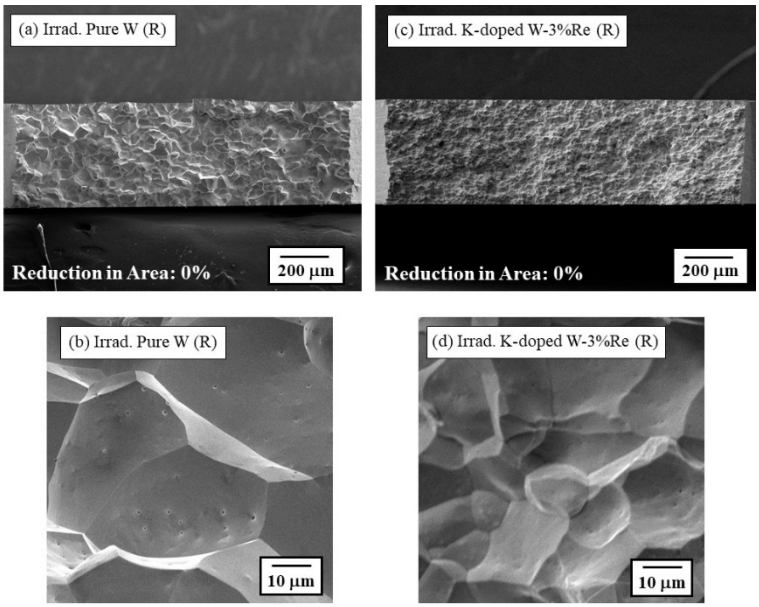

Figure 13. SEM images of the ruptured surface tested at 700 ℃ for (a) low magnification (b) high magnification in irradiated Pure W (R) and (c) low magnification (d) high magnification in irradiated K-doped W-3%Re (R). Irradiation temperatures were 810–830 ℃.

4. Discussion

In figures 4 and 9, delamination of the layered structure, introduced through rolling during their fabrication process, can be clearly observed in the K-doped W-3%Re (SR) and W-3%Re (SR) irradiated at 570–600 °C, and K-doped W-3%Re (SR) and K-doped W (SR) irradiated at 790–840 °C, evidencing ductile behavior. The reason for the delamination is because Pure W (SR) and its alloys (SR) fabricated by powder metallurgy and hot rolling have a layered structure which was formed as a result of the hot rolling process [15]. K-doped W (SR) and K-doped W-3%Re (SR) have the layered structure with finer grains than Pure W (SR). It is thought that the delamination took place along with necking deformation, also indicating that such delamination did not immediately cause specimen fracture [12]. The tensile direction of specimens was parallel to the rolling direction, therefore grains were extended in the tensile direction and thinned in a direction perpendicular to that. Since the grains became thinner as a result of the plastic and necking deformation, it could be expected that stress would therefore be generated in a direction perpendicular to the tensile direction. The triaxial stress state caused by plastic and necking deformation would trigger delamination because the grain boundaries in W are inherently weak. Mo alloys (SR) also showed similar ductile behavior, even after the high dose neutron irradiation conditions [37, 38]. Characteristic features of the neutron irradiated Mo alloys (SR) are small grain size and layered structure. Texture as a result of cold rolling may lead to the development of preferred orientation and, hence, such texture may be maintained after the stress-relief treatment. If the preferred orientation has enough binding strength between the grains in a layer, the layered structure may suppress an intergranular fracture. It was found that the stress-relief treatment and the layered structure with fine grains improved the ductility of powder-metallurgy W alloys after neutron irradiation up to 0.7 dpa.

In support of the positive effects of K-doping, grain refining with no increase in the rolling ratio, an increase in the tensile strength and the importance of ductility, especially at

lower temperatures (below DBTT), were reported [14]. The positive effects could enhance the suppression of irradiation embrittlement of SR W materials with a layered structure. However, if the layered grain structure of W materials changed the equiaxed coarse grain structure due to recrystallization, the effects of K-doping will not be applicable.

Solid solute Re in W matrix could improve not only mechanical properties but also resistance to neutron irradiation. Re addition of 3% could be effective to increase the work hardening coefficient accompanied by the increase in UE [25]. Therefore, Re addition of 3% could improve the ductility at low temperature. It was reported that solid solute Re is effective in suppressing void and dislocation loop formations [39]. Re is an under sized atom in the W matrix, therefore the substitutional Re atom has a tendency to bind self-interstitial atoms (SIA) because their lattice strain field is in opposition. Once the Re-SIA complex is formed the mobility of the SIA decreases, thus enhancing vacancy-interstitial recombination [40]. Consequently, void growth is suppressed with Re. The irradiation-induced hardening of 3%Re added W alloys was suppressed significantly in comparison to that of Pure W. In future research, the effectiveness of K-doping and Re addition will be investigated at high-temperatures, near to recrystallization temperatures, by using irradiation specimens in the 1100 ^{o}C zone (RB-19J irradiation campaign).

5. Conclusions

The irradiation hardening and tensile behavior of powder metallurgy processed, and stress-relieved (SR) or recrystallized (R) Pure W and its alloys, has been examined after neutron irradiation with a thermal neutron shield in ORNL up to 0.74 dpa at 600 °C and 800 °C. The results of this study can be concluded as follows:

The irradiation hardening of Pure W (R) irradiated in a HFIR 19J shielded capsule was smaller than that of previous data obtained from HFIR unshielded capsule irradiation. It can be suggested that irradiation hardening may be suppressed because the thermal neutron shield suppresses transmutation and irradiation-induced precipitation. Pure W (SR) showed irradiation hardening and the loss of ductility after irradiation in the 600 °C and 800 °C zones. K-doped W-3%Re (SR) also evidenced irradiation hardening and ductility after irradiation. Characteristic points of powder-metallurgy W (SR) in this study are small grain size and layered structure, introduced using rolling during the fabrication process. The grain size of K-doped W-3%Re (SR) is finer than that of Pure W (SR). The stress-relief treatment and layered structure improved the ductility of the powder-metallurgy W alloys, even after the neutron irradiation, so a combination of K-doping and Re addition is more effective in improving irradiation resistance to the powder metallurgy processed W materials. However, recrystallized K-doped W-3%Re (R) showed a loss of ductility and brittle fracture behavior even at the high temperature of 700 °C. In future work, the effectiveness of K-doping and Re addition will be investigated at higher temperatures, nearer to the recrystallization temperature.

Acknowledgement

The authors thank M. McAlister for technical support in the tensile tests. This work was performed as part of the U.S.–Japan PHENIX Collaboration Project on Technological Assessment of Plasma Facing Components for DEMO Reactors. ORNL research was sponsored by the U.S. Department of Energy, Office of Fusion Energy Sciences, under contract DE-AC05-00OR22725 with UT-Battelle, LLC. This study was supported by JSPS KAKENHI, Grant Number 17H01364.

References

[1] S. Wurster, N. Baluc, M. Battabyal, T. Crosby, J. Du, C. García-Rosales, A. Hasegawa, A. Hoffmann, A. Kimura, H. Kurishita, R.J. Kurtz, H. Li, S. Noh, J. Reiser, J. Riesch, M. Rieth, W. Setyawan, M. Walter, J.-H. You, R. Pippan, J. Nucl. Mater. 442 (2013) S181–S189.

[2] H. Bolt, V. Barabash, G. Federici, J. Linke, A. Loarte, J. Roth and K. Sato: J. Nucl. Mater. 307-311 (2002) 43-52.

[3] A.R. Raffray, R. Nygren, D.G. Whyte, S. Adbel-Khalik, R. Doerner, F. Escourbiac, T. Evans, R.J. Goldston, D.T. Hoelzer, S. Konishi, P. Lorenzetto, M. Merola, R. Neu, P. Norajitra, R.A. Pitts, M. Roedig, T. Rognlien, S. Suzuki, M.S. Tillack, C. Wong, Fusion Eng. Des. 85 (2010) 93–108.

[4] J.M. Steichen: Journal of Nuclear Materials 60 (1976) 13–19.

[5] L.R. Greenwood and F.A. Garner: J. Nucl. Mater., 212-215 (1994) 635-639.

[6] M. Fukuda, K. Yabuuchi, S. Nogami, A. Hasegawa and T. Tanaka: J. Nucl. Mater., 455 (2014) 460-463.

[7] M. Fukuda, N.A. Kiran Kumar, T. Koyanagi, L. M. Garrison, L. L Snead, Y. Katoh and A. Hasegawa: J. Nucl. Mater., 479 (2016) 249-254.

[8] T. Koyanagi, N.A. Kiran Kumar, T. Hwang, L. M. Garrison, X. Hu, L.L. Snead and Y. Katoh: J. Nucl. Mater., 490 (2017) 66-74.

[9] L. M. Garrison, Y. Katoh and N.A. Kiran Kumar: J. Nucl. Mater., 518 (2019) 208-225.

[10] L. M. Garrison, Y. Katoh, J. W. Geringer, M. Akiyoshi, X. Chen, M. Fukuda, A. Hasegawa, T. Hinoki, X. Hu, T. Koyanagi, E. Lang, M. McAlister, J. McDuffee, T. Miyazawa, C. Parish, E. Proehl, N. Reid, J. Robertson and H. Wang: Fusion. Sci. Technol., 75 (2019) 499-509.

[11] L.M. Garrison et al, ICFRM-19, (2019).

[12] K. Sasaki, K. Yabuuchi, S. Nogami and A. Hasegawa: J. Nucl. Mater., 461 (2015) 357-364.

[13] K. Sasaki, S. Nogami, M. Fukuda, Y. Katakai and A. Hasegawa: Fusion Eng. Des., 88 (2013) 1735-1738.

[14] S. Nogami, S. Watanabe, J. Reiser, M. Rieth, S. Sickinger and A. Hasegawa: Fus. Eng. Des. 140 (2019) 48-61.

[15] K. Tsuchida, T. Miyazawa, A. Hasegawa, S. Nogami and M. Fukuda: Nucl. Mater. Energy 15 (2018) 158-163.

[16] M. Fukuda, S. Nogami, A. Hasegawa, H. Usami, K. Yabuuchi and T. Muroga: Fusion Eng. Des., 89 (2014) 1033-1036.

[17] P. Schade: Int. J. Refract. Metals Hard Mater. 28 (2010) 648–660.

[18] J.W. Pugh: Metall. Trans. 4 (1973) 533–538.

[19] P.K. Wright: Metall. Trans. A 9 (1978) 955–963.

[20] D.B. Snow: Metall. Trans. A 10 (1979) 815–821.

[21] E.M. Savitskii, M.A. Tylkina, S.I. Ipatova, E.I. Pavlova: Metal Science and Heat Treatment of Metals 2 (9) (1960) 483–486.

[22] M. Fukuda, S. Nogami, K. Yabuuchi, A. Hasegawa and T. Muroga: Fusion Sci. Technol., 68 (2015) 690-693.

[23] M. Fukuda, T. Tabata, A. Hasegawa, S. Nogami and T. Muroga: Fusion Eng. Des., 109-111 (2016) 1674-1677.

[24] M. Fukuda, A. Hasegawa and S. Nogami: Fusion Eng. Des., 132 (2018) 1-6.

[25] S. Watanabe, S. Nogami, J. Reiser, M. Rieth, S. Sickinger, S. Baumgartner, T. Miyazawa and S. Hasegawa: Fusion Eng. Des., 148 (2019) 111323.

[26] J.L. McDuffee, C.R. Daily, N.O. Cetiner, C.M. Petrie and J.W Geringer, “HFIR-MFE-RB-19J Thermal and Neutronic Design,” Fusion Reactor Mater., DOE/ER-0313/60, 205 (2016).

[27] J.W. Geringer, J.L. McDuffee, C.M. Petrie, L.M. Garrison, R.H. Howard, N.O. Cetiner, D.A. Stringfield and R.G. Sitterson, “HFIR-MFE-RB-19J Specimen Loading Listing,” Fusion Reactor Mater., DOE/ER-0313/60, 215 (2016).

[28] M.E. Sawan: Fusion Eng. Des. 87 (2012) 551-555.

[29] A.A. Campbell, W.D. Porter, Y. Katoh and L.L. Snead: Nucl. Instrum. Meth. B 370 (2016) 370.

[30] T. Tanno, A. Hasegawa, J.C. He, M. Fujiwara, S. Nogami, M. Satou, et al.: Materials Transactions 48 (9) (2007) 2399–2402.

[31] M. Fukuda, T. Tanno, S. Nogami, A. Hasegawa: Materials Transactions 53 (2012) 2145–2150.

[32] A. Hasegawa, M. Fukuda, S. Nogami and K. Yabuuchi: Fus. Eng. Des. 89 (2014) 1568-1572.

[33] A. Hasegawa, M. Fukuda, T. Tanno and S. Nogami: Mater. Trans. 54 (4) (2013) 466-471.

[34] T. Tanno, M. Fukuda, S. Nogami and A. Hasegawa: Mater. Trans. 52 (7) (2011) 1447-1451.

[35] J.C. He, G.Y. Tang, A. Hasegawa and K. Abe: Nucl. Fusion 46 (2006) 877-883.

[36] Y. Katoh, L.L. Snead, L.M. Garrison, X. Hu, T. Koyanagi, C.M. Parish, P.D. Edmondson, M. Fukuda, T. Hwang, T. Tanaka and A. Hasegawa: J. Nucl. Mater. 520 (2019) 193-207.

[37] A. Hasegawa, K. Abe, M. Satou and C. Namba: J. Nucl. Mater. 225 (1995) 259-266.

[38] A. Hasegawa, K. Abe, M. Satou, K. Ueda and C. Namba: J. Nucl. Mater. 233-237 (1996) 565-569.

[39] A. Hasegawa, M. Fukuda, K. Yabuuchi and S. Nogami: J. Nucl. Mater. 471 (2016) 175-183.

[40] T. Suzudo, M. Yamaguchi and A. Hasegawa: Model. Simul. Mater. Sci. Eng. 22 (2014) 075006.